Multiple Functional Groups of Varying Ratios in Metal-Organic Frameworks

Hexiang Deng, *et al.*

Science **327**, 846 (2010);
DOI: 10.1126/science.1181761

to explore and directly image the exchange interaction and the role of conduction electrons mediating the interaction, such as the Ruderman-Kittel-Kasuya-Yosida interaction.

References and Notes

1. M. F. Crommie, C. P. Lutz, D. M. Eigler, *Science* **262**, 218 (1993).
2. J. Li, W.-D. Schneider, R. Berndt, S. Crampin, *Phys. Rev. Lett.* **80**, 3332 (1998).
3. V. S. Stepanyuk, L. Niebergall, W. Hergert, P. Bruno, *Phys. Rev. Lett.* **94**, 187201 (2005).
4. L. Niebergall, V. S. Stepanyuk, J. Berakdar, P. Bruno, *Phys. Rev. Lett.* **96**, 127204 (2006).
5. L. Niebergall *et al.*, *Phys. Rev. B* **74**, 195436 (2006).
6. M. Bode, *Rep. Prog. Phys.* **66**, 523 (2003).
7. L. Diekhöner *et al.*, *Phys. Rev. Lett.* **90**, 236801 (2003).
8. O. Pietzsch, A. Kubetzka, M. Bode, R. Wiesendanger, *Phys. Rev. Lett.* **92**, 057202 (2004).
9. O. Pietzsch *et al.*, *Phys. Rev. Lett.* **96**, 237203 (2006).
10. See supporting material on *Science* Online.
11. J. Tersoff, D. Hamann, *Phys. Rev. Lett.* **50**, 1998 (1983).
12. D. Wortmann, S. Heinze, Ph. Kurz, G. Bihlmayer, S. Blügel, *Phys. Rev. Lett.* **86**, 4132 (2001).
13. We note that the LDOS in vacuum strongly depends on the distance between the STM tip and the scanned surface (*25*).
14. J. de la Figuera, J. E. Prieto, C. Ocal, R. Miranda, *Phys. Rev. B* **47**, 13043 (1993).
15. N. N. Negulyaev *et al.*, *Phys. Rev. B* **77**, 125437 (2008).
16. F. Meier, L. Zhou, J. Wiebe, R. Wiesendanger, *Science* **320**, 82 (2008).
17. G. Rodary, S. Wedekind, D. Sander, J. Kirschner, *Jpn. J. Appl. Phys.* **47**, 9013 (2008).
18. G. Rodary, S. Wedekind, H. Oka, D. Sander, J. Kirschner, *Appl. Phys. Lett.* **95**, 152513 (2009).
19. M. V. Rastei *et al.*, *Phys. Rev. Lett.* **99**, 246102 (2007).
20. K. Wildberger, V. S. Stepanyuk, P. Lang, R. Zeller, P. H. Dederichs, *Phys. Rev. Lett.* **75**, 509 (1995).
21. We note that the spin polarization shown here is not identical with the local magnetic moment of the sample because it is obtained at a certain energy.
22. O. O. Brovko, W. Hergert, V. S. Stepanyuk, *Phys. Rev. B* **79**, 205426 (2009).
23. D. M. Eigler, E. K. Schweizer, *Nature* **344**, 524 (1990).
24. H. C. Manoharan, C. P. Lutz, D. M. Eigler, *Nature* **403**, 512 (2000).
25. J. A. Stroscio, D. T. Pierce, A. Davies, R. J. Celotta, M. Weinert, *Phys. Rev. Lett.* **75**, 2960 (1995).

26. We thank F. Donati for enlightening discussions, N. Kurowsky for expert technical support, and O. O. Brovko for carefully reading this manuscript. Supported by Deutsche Forschungsgemeinschaft grant SFB 762.

Supporting Online Material

www.sciencemag.org/cgi/content/full/327/5967/843/DC1
Materials and Methods
SOM Text
Figs. S1 to S4
References

12 October 2009; accepted 11 December 2009
10.1126/science.1183224

Multiple Functional Groups of Varying Ratios in Metal-Organic Frameworks

Hexiang Deng, Christian J. Doonan, Hiroyasu Furukawa, Ricardo B. Ferreira, John Towne, Carolyn B. Knobler, Bo Wang, Omar M. Yaghi*

We show that metal-organic frameworks (MOFs) can incorporate a large number of different functionalities on linking groups in a way that mixes the linker, rather than forming separate domains. We made complex MOFs from 1,4-benzenedicarboxylate (denoted by "A" in this work) and its derivatives -NH_2, -Br, -$(Cl)_2$, -NO_2, -$(CH_3)_2$, -C_4H_4, -$(OC_3H_5)_2$, and -$(OC_7H_7)_2$ (denoted by "B" to "I," respectively) to synthesize 18 multivariate (MTV) MOF-5 type structures that contain up to eight distinct functionalities in one phase. The backbone (zinc oxide and phenylene units) of these structures is ordered, but the distribution of functional groups is disordered. The complex arrangements of several functional groups within the pores can lead to properties that are not simply linear sums of those of the pure components. For example, a member of this series, MTV-MOF-5-EHI, exhibits up to 400% better selectivity for carbon dioxide over carbon monoxide compared with its best same-link counterparts.

Crystalline extended structures are usually considered "simple" because they are constructed from a small number of distinct building units. Attempting to increase the number of such units in solids generally leads to either mixed phases, rather than a single phase of mixed units, or amorphous materials. In block copolymers, a minor modification to the side chains alters the entropy of the system and results in major (and often undesirable) changes in the structure of the polymer (*1*). Here, we show that by combining the inherent rigidity of metal-organic frameworks (MOFs) and the functional flexibility of polymers, one can overcome these challenges and create a large number of single-phase materials, each of which has multivariate (MTV) functionalities.

California Nanosystems Institute, University of California–Los Angeles (UCLA)–Department of Energy (DOE) Institute of Genomics and Proteomics, Department of Chemistry and Biochemistry, UCLA, 607 Charles E. Young Drive East, Los Angeles, CA 90095, USA.

*To whom correspondence should be addressed. E-mail: yaghi@chem.ucla.edu

Our strategy to making MTV-MOFs is to assemble their structures from links with different functional groups whose orientation, number, relative position, and ratio along the backbone (metal-oxide and phenylene units) can be controlled by virtue of the unchanged length of the link and its unaltered connectivity (Scheme 1). Such a construct can be viewed as having a primary structure composed of the simple repeating pattern of metal-oxide joints and organic links and a "complex" secondary structure formed by multivaried arrangements of many functional groups that are covalently bound to the links. In this way, each of the pores within the MOF would have an array of functionalities pointing into its center. Accordingly, the sequence of such functionalities and the frequency with which certain ones appear in the sequence will endow the pores with a new level of complexity that far exceeds any held by that of the original same-link MOFs—an aspect that may allow fine-tuning of the pore environment with favorable implications on properties.

Our past work (as well as the work of others) has shown that MOFs with two mixed links can be prepared, whereas a recent report showed that four different functionalities can be introduced into one structure by post-synthesis modification (*2*–*7*). These approaches are either confined to only two links or severely limited by having complete reactions at the links; multiple variations in link ratios and functionalities in these systems were not demonstrated. The present report describes a general method for producing crystalline MOF materials that combine sets of two to eight links of different functional groups; each set is incorporated into a single structure where the ratio of links is controlled, and the material can be produced with bulk purity. [Hereafter, A, 1,4-benzenedicarboxylate; B, -NH_2; C, -Br; D, -$(Cl)_2$; E, -NO_2; F, -$(CH_3)_2$; G, -C_4H_4; H, -$(OC_3H_5)_2$; and I, -$(OC_7H_7)_2$.] Specifically, we targeted the cubic MOF-5 structure (*8*) and combined the acid form of 1,4-benzenedicarboxylate (BDC), NH_2-BDC, Br-BDC, $(Cl)_2$-BDC, NO_2-BDC, $(CH_3)_2$-BDC, C_4H_4-BDC, $(OC_3H_5)_2$-BDC, and $(OC_7H_7)_2$-BDC links (Scheme 2, A to I, respectively) to form the corresponding sets of 18 MTV-MOFs, each having two or more different functionalities [two: MTV-MOF-5-AB, -AC, -AD, -AE, -AF, -AG, -AH, -AI, and -EI; three: MTV-MOF-5-ABC, -AHI, and -EHI; four: MTV-MOF-5-ABCD and -ACEF; five: MTV-MOF-5-ABCHI; six: MTV-MOF-5-ABCGHI; seven: MTV-MOF-5-ABCEGHI; eight: MTV-MOF-5-ABCEFGHI (Scheme 2)]. We describe their isolation as single phases, the structure of their MOF backbone, and their porosity, and show that this multivaried link synthetic strategy is useful for introducing functionalities [such as NO_2-BDC and $(Cl)_2$-BDC] into the MOF-5 type structure (MTV-MOF-5-AD and -AE) that do not form this structure when used alone. We also report our initial findings that members of this series (MTV-MOF-5-AHI and -EHI) show that the "whole is better than the sum of its parts," as evidenced by the fourfold enhancement of gas adsorption and separation properties of the multivaried

link MOFs compared with their simple same-link analogs.

Crystals of MTV-MOFs were obtained by adding $Zn(NO_3)_2 \cdot 4H_2O$ to a *N*,*N*-dimethylformamide solution mixture of the acid form of the selected organic links under conditions previously used in the synthesis of MOF-5 (*8*, *9*). All of the compounds were characterized by powder x-ray diffraction (PXRD), ^{13}C cross-polarization/magic angle spinning nuclear magnetic resonance (^{13}C CP/MAS NMR), ^{1}H NMR on acid-digested solutions of their crystals, and thermogravimetric analysis (TGA) to assess their crystallinity, link composition, link ratio, and thermal stability, respectively. The porosity of a subset of these compounds (all containing two, three, or four different links, and MTV-MOF-5-ABCEFGHI) was evaluated by nitrogen gas adsorption measurements. Although we present the complete characterization procedure and the data acquired on all of the compounds (*10*), here we describe the particulars of MTV-MOF-5-ABCD as an illustrative example. The compound was synthesized from equimolar amounts of link A, B, C, and D. Its high crystallinity was evident from the PXRD pattern of the as-synthesized samples, which gave sharp diffraction lines matching those of the parent MOF-5 structure (Fig. 1A). To determine the ratio of the four types of links in MTV-MOF-5-ABCD, the sample was evacuated by heating at 50°C under vacuum (10 mTorr) for 24 hours to remove any guest solvent molecules from the pores that were occluded during synthesis (*10*). TGA performed on this sample showed no weight loss up to 400°C, confirming that all guest molecules were removed from the pores and that the evacuated framework is thermally stable.

^{13}C CP/MAS NMR spectra of evacuated samples of MTV-MOF-5-ABCD showed resonances at 150.3, 127.0, 133.7, and 136.3 parts per million (ppm), characteristic of the unique carbon atoms of NH_2-BDC, Br-BDC, $(Cl)_2$-BDC, and BDC links, respectively (Fig. 1B). These spectra indicate the presence of these units in the MOF backbone. Additionally, the same experiment was performed on a mixture of the constituent free links of MTV-MOF-5-ABCD, where a distinct shift of 2 ppm was observed between the carbonyl carbons of the free links and those of the links that are incorporated into the framework, thus confirming that no unbound organic link is present within the MOF crystals. Similar analyses on all the remaining MTV-MOFs led to the same conclusion (*10*).

The precise link ratio was obtained from the ^{1}H NMR spectra of a DCl-digested solution of the MTV-MOF-5-ABCD solid (Table 1, link composition). Resonances with the predicted coupling patterns were observed in the expected regions for each of the unique protons of the links (Fig. 1C) (*10*). By integrating resonance peak intensities, we find that the

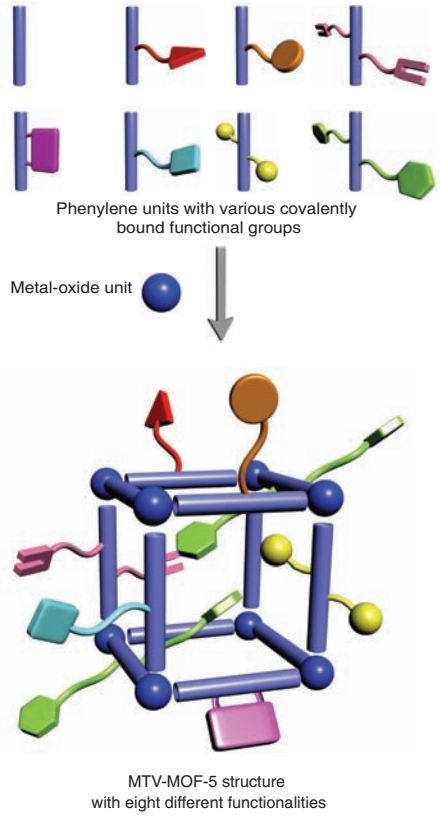

Scheme 1.

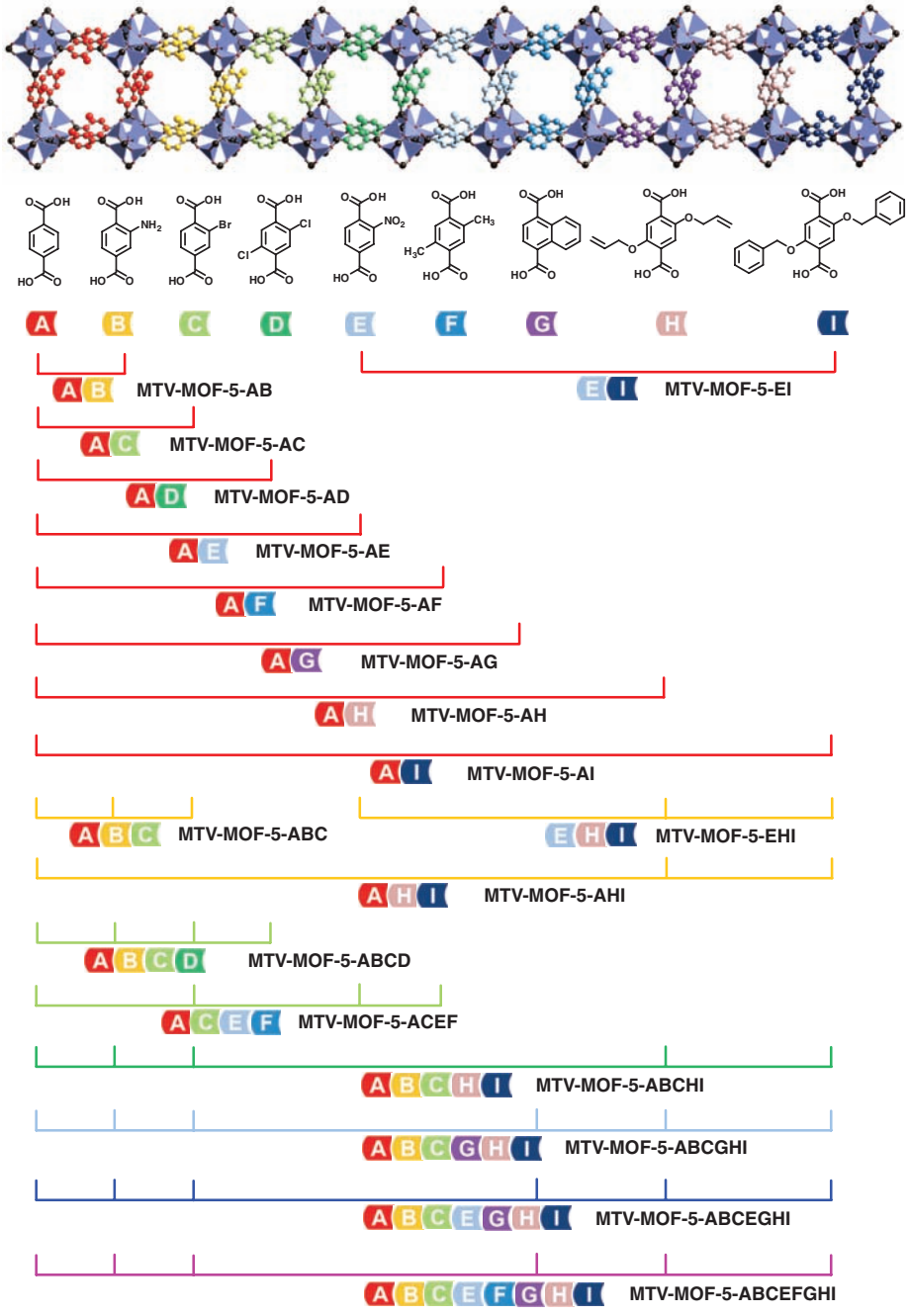

Scheme 2.

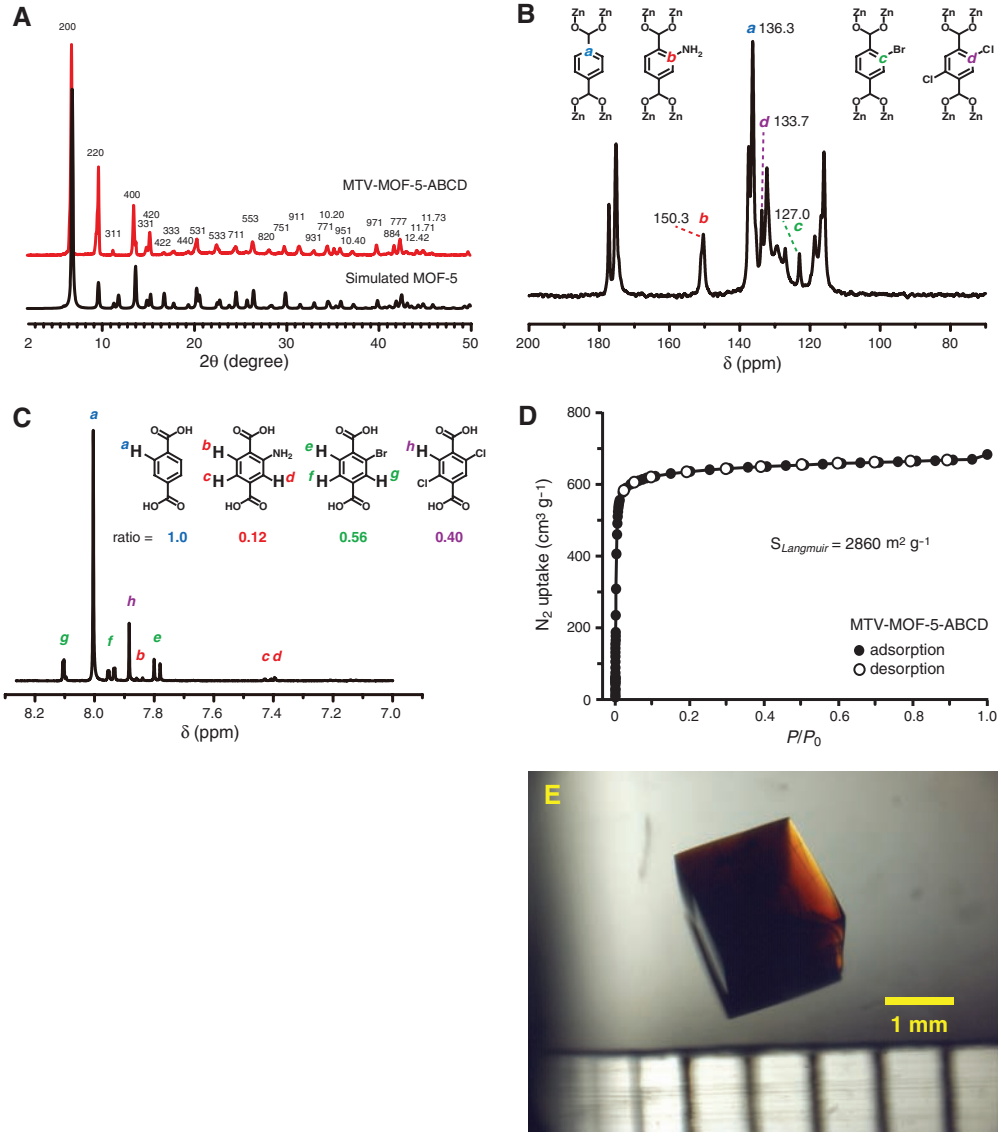

Fig. 1. Typical analysis performed on MTV-MOFs shown here for samples of MTV-MOF-5-ABCD. (**A**) X-ray diffraction patterns of the crystalline powder compared with the simulated one for MOF-5. (**B**) ^{13}C CP/MAS NMR spectrum showing unique resonance for each link. (**C**) Solution ^{1}H NMR spectrum used to determine the ratio of links (A: B: C: D = 1.0: 0.12 ± 0.03: 0.56 ± 0.04: 0.40 ± 0.03). (**D**) N_2 adsorption isotherm at 77 K with adsorption and desorption points represented by closed circles and open circles, respectively. $S_{Langmuir}$, Langmuir surface area; P/P_0, relative pressure. (**E**) A large crystal from which segments were analyzed for the ratio of links and found to be identical throughout.

links are present in the MOF in the proportion 1.00: 0.12: 0.56: 0.40 (A: B: C: D, respectively), versus an equimolar starting pool. Solution ^{1}H NMR experiments on four different crystals randomly selected from the MTV-MOF-5-ABCD bulk sample and showed that the ratios stay nearly identical. The same experiment was also performed on MTV-MOF-5-AB and -ABCEFGHI, again confirming the bulk homogeneity of the MTV-MOF series (table S1). Furthermore, the porosity and architectural stability of the original MOF-5 structure are preserved in the MTV-MOF compounds (*10*), as illustrated by the type I nitrogen adsorption isotherm (shown in Fig. 1D for MTV-MOF-5-ABCD) and its high surface area (2860 $m^2\ g^{-1}$). In addition, by synthesizing MTV-MOF-ABCD, we used a variety of link molar ratios to demonstrate that, in a given MTV-MOF, the link ratio can be controlled by modifying the reaction stoichiometry (Table 1, control of link ratio). In essence, this type of control in link ratios translates into control of the population and diversity of functional groups pointing into the pores without altering the underlying connectivity of the primary structure, as evidenced by their preserved PXRD patterns (fig. S40).

As expected, x-ray crystallographic studies performed on single crystals of MTV-MOF-5-AC and -ACEF revealed an ordered cubic MOF-5 structure composed of rigid phenylene units joined by $Zn_4O(CO_2)_6$ vertices. The nonhydrogen atoms of the functional groups on the phenylene units in these materials are all present at very low occupancy. Each functional group is required by symmetry to be disordered over two (dimethyl groups of link F) or four (Br group of link C or nitro group of link E) positions because of an equal probability of their location on the four carbon atoms of the phenylene ring. Parameters for Br in MTV-MOF-5-AC can be refined, despite its low occupancy and the low contribution to the intensity of the data. In MTV-MOF-5-ACEF, the occupancies of functional group atoms are also quite low; however, because there is overlap of the positions of Br (link C), N (link E), and C (link F) atoms, a difference peak could be located. Given that phenylene unit atoms are present in all MTV-MOFs, all of these parameters were successfully refined for the backbone nonhydrogen atoms. This result indicates that the structures of MTV-MOFs are not solid solutions. Thus, they represent a unique crystalline material in which a variable distribution of functional groups is covalently linked to an ordered framework.

The x-ray analysis cannot address whether the crystals are composed of macroscopic domains of functionalities or whether they have distinct sequences of functional units repeated throughout the framework backbone. To distinguish these two possibilities, we prepared large single crystals of MTV-MOF-5-AB, -ABCD (Fig. 1E), and -ABCEFGHI of dimensions of 4.0 mm by 4.0 mm by 2.0 mm, 2.0 mm by 2.0 mm by 2.0 mm, and 2.0 mm by 2.0 mm by 1.0 mm, respectively (fig. S33). In each case, the structure of each single crystal was confirmed by its x-ray diffraction pattern (figs. S34 to S36). Each crystal was dissected into three equal segments,

Table 1. Ratio of links determined for MTV-MOF crystals and their respective reaction stoichiometry (shown in parentheses). In each case, the ratios were normalized to a value of one for link A. NA, not applicable.

Compound	A, (A)	B, (B)	C, (C)	D, (D)	E, (E)	F, (F)	G, (G)	H, (H)	I, (I)
				Link composition					
MTV-MOF-5-AB	1.0, (1)	0.57, (1)	NA	NA	NA	NA	NA	NA	NA
MTV-MOF-5-AC	1.0, (1)	NA	0.61, (1)	NA	NA	NA	NA	NA	NA
MTV-MOF-5-AD	1.0, (1)	NA	NA	0.63, (1)	NA	NA	NA	NA	NA
MTV-MOF-5-AE	1.0, (1)	NA	NA	NA	0.40, (1)	NA	NA	NA	NA
MTV-MOF-5-AF	1.0, (1)	NA	NA	NA	NA	1.24, (1)	NA	NA	NA
MTV-MOF-5-AG	1.0, (1)	NA	NA	NA	NA	NA	0.52, (1)	NA	NA
MTV-MOF-5-AH	1.0, (1)	NA	NA	NA	NA	NA	NA	0.46, (1)	NA
MTV-MOF-5-AI	1.0, (1)	NA	NA	NA	NA	NA	NA	NA	0.40, (1)
MTV-MOF-5-EI*	NA	NA	NA	NA	0.20, (1)	NA	NA	NA	1, (1)
MTV-MOF-5-ABC	1.0, (1)	0.052, (1)	0.52, (1)	NA	NA	NA	NA	NA	NA
MTV-MOF-F-AHI	1.0, (1)	NA	NA	NA	NA	NA	NA	0.48, (1)	0.50, (1)
MTV-MOF-5-EHI*	NA	NA	NA	NA	0.62, (1)	NA	NA	0.89, (1)	1, (1)
MTV-MOF-5-ABCD	1.0, (1)	0.12, (1)	0.56, (1)	0.40, (1)	NA	NA	NA	NA	NA
MTV-MOF-5-ACEF	1.0, (1)	NA	0.49, (1)	NA	0.22, (1)	0.62, (1)	NA	NA	NA
MTV-MOF-5-ABCHI	1.0, (1)	0.017, (1)	0.22, (1)	NA	NA	NA	NA	0.62, (1)	0.32, (1)
MTV-MOF-5-ABCGHI	1.0, (1)	0.093, (1)	0.87, (1)	NA	NA	NA	0.67, (1)	0.73, (1)	0.80, (1)
MTV-MOF-5-ABCEGHI	1.0, (1)	0.077, (1)	1.0, (1)	NA	0.69, (1)	NA	0.77, (1)	0.73, (1)	0.96, (1)
MTV-MOF-5-ABCEFGHI	1.0, (1)	0.14, (1)	0.56, (1)	NA	0.29, (1)	0.67, (1)	0.56, (1)	0.48, (1)	0.56, (1)
				Control of link ratio					
MTV-MOF-5-ABCD-a	1.0, (1)	0.12, (1)	0.56, (1)	0.40, (1)	NA	NA	NA	NA	NA
MTV-MOF-5-ABCD-b	1.0, (0.5)	0.26, (1)	1.24, (1)	1.99, (1.5)	NA	NA	NA	NA	NA
MTV-MOF-5-ABCD-c	1.0, (1.5)	0.06, (1)	0.43, (1)	0.30, (0.5)	NA	NA	NA	NA	NA
MTV-MOF-5-ABCD-d	1.0, (1)	0.32, (1.5)	0.26, (0.5)	0.44, (1)	NA	NA	NA	NA	NA
MTV-MOF-5-ABCD-e	1.0, (1)	0.03, (0.5)	1.0, (1.5)	0.67, (1)	NA	NA	NA	NA	NA

*Numerical value of link E was normalized to 1.

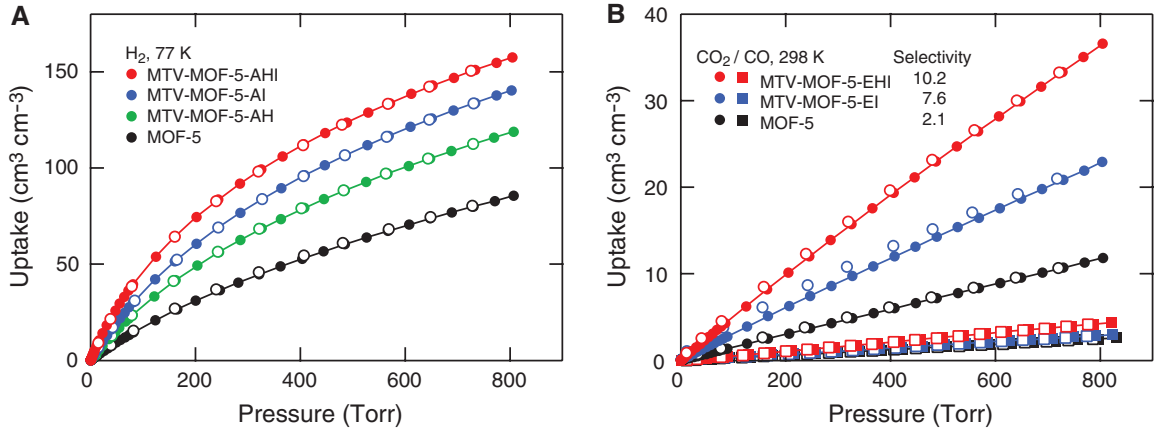

Fig. 2. (**A**) H_2 adsorption isotherm at 77 K of MTV-MOF-5-AH (green), -AI (blue), -AHI (red), and MOF-5 (black). (**B**) CO_2 (circles) and CO (squares) adsorption isotherms at 298 K of MTV-MOF-5-EI (blue), -EHI (red), and MOF-5 (black). Adsorption and desorption branches are represented by closed and open circles for CO_2 (closed and open squares for CO), respectively. Instrumental uncertainty is ± 5%.

and then the solution ^{1}H NMR spectra were collected on acid-digested samples of each segment of each crystal. If macroscopic domains of homogeneous links were present within a single crystal of the MTV-MOF, a different link ratio would be expected for each of the three segments of the respective parent crystal. However, the data show that the link distribution ratios are identical for each segment of the three MTV-MOFs studied (table S2), which suggests the absence of macroscopic domains. Further evidence supporting this conclusion is the absence of a narrow pore-size distribution for MTV-MOF-5-AI as one would observe for MOF-5 (*9*) or any other same-link MOF, which suggests that link I is distributed throughout the pores (*10*). This analysis does not preclude the presence of microscopic domains where one might expect the dominance of a specific functionality (or a subset of functionalities) over the nanometer scale. We believe that the combination of the NMR experiments and pore size distribution analysis strongly support the absence of large domains (greater than a nanometer scale) of homogeneous links within the crystal. Our reasoning is that the most likely bias for one functionality versus another would originate from steric interactions between proximal functional groups covalently bound to the *ortho*-carbon atoms of adjacent links at the $Zn_4O(CO_2)_6$ vertices. Accordingly, two functionalities with disfavored interaction may not be found next to each other but would probably be accommodated separately within adjacent unit cells. These effects favor small domains (if any) and point to the possibility that the functionalities might be arranged in a specific sequence determined by the energy of functional group interactions. Evidence for this rationale is indicated by the

observed link ratios of those MTV-MOFs synthesized from an equimolar ratio of links involving the most sterically unencumbered link A, where a disproportionately higher amount of link A is retained in the resulting MTV-MOFs (Table 1).

The possible presence of distinct sequences of functionalities along the MOF backbone would inevitably lead to a complex pore environment and provide opportunities for uncovering unusual properties. Because the same-link MOF-5 structure can take up large amounts of gases (for example, H_2, CO_2) (*8*, *11*–*13*), we sought to test the MTV-MOFs in these applications and to determine whether their performance is greater than that of their constituents. In Fig. 2A, we compare the H_2 storage capacities of MTV-MOF-5-AHI, -AH, -AI, and MOF-5. The isotherms demonstrate that the uptake capacity of MTV-MOF-5-AHI is greater than that of MTV-MOF-5-AH, -AI, and -A (MOF-5) by a maximum of 84%. Similarly, an unusual increase in the selective uptake capacity of CO_2 over CO was observed: 400% better selectivity in the case of MTV-MOF-5-EHI for CO_2 compared with MOF-5 (*4*, *14*, *15*) (Fig. 2B). These findings demonstrate that the properties of MTV-MOFs are not simple linear combinations of their constituents, thus supporting the notion that the sequence of functionalities within MTV-MOF may very well be useful as code for the enhancement of a specific property or achieving a new property.

References and Notes

1. S. B. Darling, *Prog. Polym. Sci.* **32**, 1152 (2007).
2. R. Kitaura, K. Fujimoto, S. Noro, M. Kondo, S. Kitagawa, *Angew. Chem. Int. Ed.* **41**, 133 (2002).
3. K. Kumazawa, K. Biradha, T. Kusukawa, T. Okano, M. Fujita, *Angew. Chem. Int. Ed.* **42**, 3909 (2003).
4. R. Banerjee *et al.*, *Science* **319**, 939 (2008).
5. K. Koh, A. G. Wong-Foy, A. J. Matzger, *Angew. Chem. Int. Ed.* **47**, 677 (2008).
6. A. D. Burrows, C. G. Frost, M. F. Mahon, C. Richardson, *Angew. Chem. Int. Ed.* **47**, 8482 (2008).
7. S. J. Garibay, Z. Wang, K. K. Tanabe, S. M. Cohen, *Inorg. Chem.* **48**, 7341 (2009).
8. H. Li, M. Eddaoudi, M. O'Keeffe, O. M. Yaghi, *Nature* **402**, 276 (1999).
9. M. Eddaoudi *et al.*, *Science* **295**, 469 (2002).
10. See supporting online material on *Science* Online.
11. N. L. Rosi *et al.*, *Science* **300**, 1127 (2003).
12. S. S. Kaye, A. Dailly, O. M. Yaghi, J. R. Long, *J. Am. Chem. Soc.* **129**, 14176 (2007).
13. A. R. Millward, O. M. Yaghi, *J. Am. Chem. Soc.* **127**, 17998 (2005).
14. R. Banerjee *et al.*, *J. Am. Chem. Soc.* **131**, 3875 (2009).
15. Single-link MOFs of links H and I, respectively, were synthesized and found to be nonporous. Furthermore, we were unable to synthesize a single-link MOF from link E; thus, CO_2/CO separation data for these compounds was not included in our comparison.

16. This work was supported by DOE Office of Basic Energy Sciences (grant DE-FG02-08ER15935). We thank F. J. Uribe-Romo and R. Taylor for assistance and helpful discussions. MTV-MOF-5-AC and MTV-MOF-5-ACEF have been deposited into the Cambridge Crystallographic Data Centre (CCDC) under deposition numbers CCDC 747004 to 747007.

Supporting Online Material

www.sciencemag.org/cgi/content/full/327/5967/846/DC
Materials and Methods
Figs. S1 to S52
Tables S1 to S20
References

10 September 2009; accepted 30 November 2009
10.1126/science.1181761

Break-Up of Stepped Platinum Catalyst Surfaces by High CO Coverage

Feng Tao,[1,2] Sefa Dag,[3] Lin-Wang Wang,[3] Zhi Liu,[4] Derek R. Butcher,[1,2] Hendrik Bluhm,[4,5] Miquel Salmeron,[1,6]* Gabor A. Somorjai[1,2]*

Stepped single-crystal surfaces are viewed as models of real catalysts, which consist of small metal particles exposing a large number of low-coordination sites. We found that stepped platinum (Pt) surfaces can undergo extensive and reversible restructuring when exposed to carbon monoxide (CO) at pressures above 0.1 torr. Scanning tunneling microscopy and photoelectron spectroscopy studies under gaseous environments near ambient pressure at room temperature revealed that as the CO surface coverage approaches 100%, the originally flat terraces of (557) and (332) oriented Pt crystals break up into nanometer-sized clusters and revert to the initial morphology after pumping out the CO gas. Density functional theory calculations provide a rationale for the observations whereby the creation of increased concentrations of low-coordination Pt edge sites in the formed nanoclusters relieves the strong CO-CO repulsion in the highly compressed adsorbate film. This restructuring phenomenon has important implications for heterogeneous catalytic reactions.

Industrial catalysts usually consist of small particles exposing different atomic terminations that exhibit a high concentration of step edges, kink sites, and vacancies at the edge of the facets, which are thought to be the catalytically active sites (*1*–*3*). Stepped single-crystal surfaces with well-defined surface structures can be prepared with a high density of such sites. They are models of real catalysts because vicinal surfaces mimic closely the rough regions of the catalyst surface.

Adsorbates are known to induce structural changes, known as reconstructions in surface science. Steps are particularly notable for being modified when adsorbates bind to the surface. These are phenomena well known in vacuum surface science (*4*–*6*). The present work deals with more profound changes, driven by the formation of dense adsorbate layers. These can be formed when the adsorption energy is high—for example, when oxygen adsorbs and initiates the oxidation process. When the adsorption energy is weaker, however, dense layers can only be formed under reaction conditions of high reactant pressures near or above room temperature.

Real catalysts operate under pressures ranging from millitorr to atmospheres and from room temperature to hundreds of degrees Celsius, so that the surfaces can easily change and adopt the structure corresponding to thermodynamic equilibrium. However, most surface science experiments are usually performed under high vacuum where the high adsorbate coverage characteristic of working catalysts cannot be attained unless the samples are kept at low temperature. These conditions will likely inhibit any restructuring process that requires overcoming of even moderate activation barriers. Thus, to understand catalytic processes at the atomic and molecular level, it is crucial to explore the structural and chemical evolution of catalyst surfaces under reaction conditions.

The limitations of traditional surface science techniques can be overcome with the use of techniques that operate under realistic conditions (*7*–*13*), including high-pressure scanning tunneling microscopy (STM) and ambient pressure x-ray photoelectron spectroscopy (AP-XPS). With these two techniques, we can image the atomic structure and identify the chemical state of catalyst atoms and adsorbed reactant molecules under realistic conditions. Here we concentrate on carbon monoxide (CO), a reactant in many important industrial catalytic processes, such as Fischer-Tropsch synthesis of hydrocarbons (*14*, *15*), CO oxidation in automobile catalytic converters (*16*, *17*), and degradation of Pt electrodes in hydrogen fuel cell processes (*18*–*20*).

Our studies revealed an unexpected and reversible large-scale restructuring of the surfaces of two Pt stepped surfaces, Pt(557) and Pt(332), both of which consist of six-atoms-wide terraces of (111) orientation separated by monoatomic steps of different orientation. On Pt(557) the step atoms form a (100)-type square cell, whereas on Pt(332) they form a (111)-type triangular cell (fig. S1) (*21*). Under high coverage of CO, these flat terraces break up into an array of nanoclusters

[1]Materials Science Division, Lawrence Berkeley National Lab, Berkeley, CA 94720, USA. [2]Department of Chemistry, University of California, Berkeley, CA 94720, USA. [3]Computational Research Division, Lawrence Berkeley National Lab, Berkeley, CA 94720, USA. [4]Advanced Light Source, Lawrence Berkeley National Lab, Berkeley, CA 94720, USA. [5]Chemical Science Division, Lawrence Berkeley National Lab, Berkeley, CA 94720, USA. [6]Department of Materials Science and Engineering, University of California, Berkeley, CA 94720, USA.

*To whom correspondence should be addressed. E-mail: somorjai@berkeley.edu (G.A.S.); mbsalmeron@lbl.gov (M.S.)